Far from equilibrium dynamics of tracer particles embedded in a growing multicellular spheroid

Himadri S. Samanta,[1] Sumit Sinha,[2] and D. Thirumalai[1]

[1]*Department of Chemistry, University of Texas at Austin, TX 78712*
[2]*Department of Physics, University of Texas at Austin, TX 78712*

(Dated: March 28, 2020)

By embedding inert tracer particles (TPs) in a growing multicellular spheroid the local stresses on the cancer cells (CCs) can be measured. In order for this technique to be effective the unknown effect of the dynamics of the TPs on the CCs has to be elucidated to ensure that the TPs do not greatly alter the local stresses on the CCs. We show, using theory and simulations, that the self-generated (active) forces arising from proliferation and apoptosis of the CCs drive the dynamics of the TPs far from equilibrium. On time scales less than the division times of the CCs, the TPs exhibit sub-diffusive dynamics (the mean square displacement, $\Delta_{TP}(t) \sim t^{\beta_{TP}}$ with $\beta_{TP} < 1$), similar to glass-forming systems. Surprisingly, in the long-time limit, the motion of the TPs is hyper-diffusive ($\Delta_{TP}(t) \sim t^{\alpha_{TP}}$ with $\alpha_{TP} > 2$) due to persistent directed motion for long times. In comparison, proliferation of the CCs randomizes their motion leading to superdiffusive behavior with α_{CC} exceeding unity. Most importantly, α_{CC} is not significantly affected by the TPs. Our predictions could be tested using *in vitro* imaging methods where the motion of the TPs and the CCs can be tracked.

PACS numbers:

The interplay of systematic short-range forces and non-equilibrium processes arising from cell division and apoptosis give rise to unexpected dynamics in the collective migration of cancer cells [1–7]. An example of relevance here is the invasion of cancer cells (CCs) in a growing multicellular spheroid (MCS), which is relevant in cancer metastasis [6, 7]. Imaging experiments show that the cell dynamics, characterized by a group of cells that remain in contact for a long period, is complex manifesting far from equilibrium characteristics [7–11]. Simulations and theory of minimal models have been used to describe some of the unexpected features observed in the experiments [12–15]. These studies have also established that the dynamics of a growing tumor embedded in an extracellular matrix are spatially highly heterogeneous. The cells in the interior of the solid tumor spheroid undergo sluggish glass-like dynamics whereas those far from the center of the tumor undergo directed faster than diffusive motion [15]. It should be pointed out that explicit introduction of stochastic active forces could also give rise to unusual dynamics in abiotic systems [16–18].

The dynamics of CCs in a growing tumor is determined by the effects of the CC microenvironment on the long time collective migration. The advent of new experimental techniques that probe the local stresses or pressure on the CCs [19–24] have provided insights into the mechanism by which the CCs invade the extracellular matrix. In a recent article, Dolega et. al. [24] developed a method to measure the mechanical stress within MCSs by embedding micron-sized inert deformable polyacrylamide beads (elastic and compressible hydrogel micro-beads) as local stress sensors. The local pressure profiles in the MCS were extracted from the volume changes in the randomly distributed beads by applying osmotic stress. Surprisingly, it was found that the pressure drops at the surface of the spheroid and increases close to the core of the spheroid.

Inspired in part by this experiment, we used theory and simulations to extract the non-equilibrium collective cell movement during the MCS expansion by following the dynamics of the embedded inert tracer particles (TPs). In our model, a CC grows till it reaches a critical size whereupon it divides into two at a rate k_b. In addition, a randomly chosen CC could undergo apoptosis at a rate, k_a, which is less than k_b. The inequality ($k_a < k_b$), chosen to mimic tumor growth, gives rise to self-generated active forces, making the tumor growth far from equilibrium process [25]. We model the CCs and TPs as deformable objects subject to short-ranged repulsive elastic forces arising from other CCs and TPs, and adhesive attractions involving neighboring CCs and TPs. We investigated the relevant continuum description of the collective behavior of a colony of tracers in the finite as well as in the long time limit, using the Parisi-Wu stochastic quantization method [13, 26–28].

The central results of this study are : (1) The theoretical results show theory that the TPs exhibit sub-diffusive motion in the intermediate time scale ($t \lesssim \frac{1}{k_b}$), with the mean squared displacement, $\Delta_{TP}(t) \sim t^{\beta^T_{TP}}$, with $\beta^T_{TP} = \frac{4}{7}$. In the long time limit, ($t \gtrsim \frac{1}{k_b}$), the TPs undergo hyper-diffusive motion, $\Delta_{TP}(t) \sim t^{\alpha^T_{TP}}$ with $\alpha^T_{TP} = \frac{16}{7}$, in three dimensions. Surprisingly, the value of α_{TP} depends on the form of the short-range interactions between the TPs and CCs, and hence is not universal. (2) In the long time limit, the extent of migration of the TPs relative to CCs is greater, which is reflected in higher α_{TP} compared to CCs, $\alpha_{CC} = 1.45$. The values of both α_{TP} and α_{CC}, obtained using simulations, which uses entirely different forms for the interactions involving both CCs and TPs, are in quantitative agreement with the

theoretical predictions. In contrast, the simulation value for $\beta^S_{TP}(= 0.11)$ is less than the theoretical predictions, likely reflecting substantial differences in the short-range interactions. (3) The dynamics of the CCs and TPs in the intermediate time regime change only quantitatively as the size of the TPs increase. Remarkably, the long time exponents (α_{TP} and α_{CC}) are unaffected as the size of the inert probe particles is increased. This implies that the dynamics of the CCs can be faithfully recovered by following the time-dependent changes in the positions of the TPs, in principle is possible using imaging experiments.

Theory: We assume that the TP and CC dynamics are governed by stochastic equations. The inert (do not divide or undergo apoptosis) but deformable TPs in a growing tumor spheroid experience systematic short-range volume exclusion interactions arising from other TPs and the CCs. In addition, they are also subject to a random force characterized by Gaussian white noise. The inter CC interactions are modeled by a sum of attractive and repulsive excluded interactions [13]. In order to derive expressions for the mean square displacements, we first obtain an equation for the CC density in terms of $\phi_i(\mathbf{r},t) = \delta[\mathbf{r} - \mathbf{r_i(t)}]$, and the TP density $\psi_i(\mathbf{r},t) = \delta[\mathbf{r} - \mathbf{r_i(t)}]$. A closed form Langevin equation for the CC density, $\phi(\mathbf{r},t) = \sum_i \phi_i(\mathbf{r},t)$, and the density of TPs ($\psi(\mathbf{r},t) = \sum_i \psi_i(\mathbf{r},t)$) may be obtained using the Dean's method [29]. The time evolutions of $\phi(\mathbf{r},t)$ and $\psi(\mathbf{r},t)$ are given by,

$$\frac{\partial\psi(\mathbf{r},t)}{\partial t} = D_\psi\nabla^2\psi(\mathbf{r},t) + \nabla\cdot\left(\psi(\mathbf{r},t)\int_{\mathbf{r}'}[\psi(\mathbf{r}',t)+\phi(\mathbf{r}',t)]\nabla U(\mathbf{r}-\mathbf{r}')\right) + \tilde{\eta}_\psi, \tag{1}$$

$$\frac{\partial\phi(\mathbf{r},t)}{\partial t} = D_\phi\nabla^2\phi(\mathbf{r},t) + \nabla\cdot\left(\phi(\mathbf{r},t)\int_{\mathbf{r}'}[\psi(\mathbf{r}',t)+\phi(\mathbf{r}',t)]\nabla U(\mathbf{r}-\mathbf{r}')\right) + k_a\phi(\frac{k_b}{k_a}-\phi) + \sqrt{k_b\phi + k_a\phi^2}f_\phi + \tilde{\eta}_\phi \tag{2}$$

where $\tilde{\eta}_\psi(\mathbf{r},t) = \nabla\cdot\left(\eta_\psi(\mathbf{r},t)\psi^{1/2}(\mathbf{r},t)\right)$, $\tilde{\eta}_\phi(\mathbf{r},t) = \nabla\cdot\left(\eta_\phi(\mathbf{r},t)\phi^{1/2}(\mathbf{r},t)\right)$, and $\eta_{\phi,\psi}$ satisfies $<\eta_{\phi,\psi}(\mathbf{r},t)\eta_{\phi,\psi}(\mathbf{r}',t')>= \delta(\mathbf{r}-\mathbf{r}')\delta(t-t')$. The second term in Eq.(1) accounts for the TP-TP interactions $(\nabla\cdot\left(\psi(\mathbf{r},t)\int_{\mathbf{r}'}\psi(\mathbf{r}',t)\nabla U(\mathbf{r}-\mathbf{r}')\right))$ and TP-CC interactions, $(\nabla\cdot\left(\psi(\mathbf{r},t)\int_{\mathbf{r}'}\phi(\mathbf{r}',t)\nabla U(\mathbf{r}-\mathbf{r}')\right))$. The influence of the CCs on the TP dynamics occurs explicitly through the TP-CC coupling. We show below and in more detail in the Supplementary Information (SI) that these two non-linear terms determine the scaling behavior of the dynamical observables for the TPs in both the finite and the long time limit. Similarly, the second term in Eq.(2) contains the CC-CC ($\phi\phi$ fields) and CC-TP interaction ($\phi\psi$) fields.

Because we are interested in the dynamics of the TPs in a growing MCS, we modified the density evolution equation for the CCs phenomenologically by adding a non-linear source term, $\propto \phi(\phi_0 - \phi)$, representing the biological cell birth and apoptosis processes (third term in Eq.(2)), and a non-equilibrium noise term (fourth term in Eq.(2)) that breaks the number conservation of the CCs. The noise, f_ϕ, satisfies $< f_\phi(\mathbf{r},t)f_\phi(\mathbf{r}',t')>= \delta(\mathbf{r}-\mathbf{r}')\delta(t-t')$. The source term, $\propto \phi(\phi_0-\phi)$, represents the birth and apoptosis events, with $\phi_0 = \frac{k_b}{k_a}$[30, 31]. The coefficient of f_ϕ, $\sqrt{k_b\phi + k_a\phi^2}$, is the strength of the noise corresponding to number fluctuations, which is a function of the CC concentration. This form has been derived previously [32] using well known methods [33, 34].

Because the equation (Eq. 1), describing the collective motility of the TPs coupled with CCs, violates the fluctuation-dissipation theorem (FDT) due to self-generated forces arising from birth and apoptosis processes, we use the Parisi-Wu [26] stochastic quantization method to calculate the dynamics of the TPs and CCs. To characterize the dynamics of the TPs, we introduce a fictitious time 'τ_f', and consider the density and noise fields to be functions of τ_f in addition to the parameters, $\mathbf{r}$ and t. The dynamics in the fictitious time (Eq. (S6) in the SI) requires only the calculation of the response function (G). In this formalism, the correlation function, C is related to G through the FDT relation, which in Fourier space reads, $C = \frac{1}{\omega_{\tau_f}}\text{Im } G$. We can obtain the scaling laws in real space and time from the solution of the density fields in the fictitious time 'τ_f' variable.

We obtain the following self-consistent equation for the self energy (defined in Eq. (S9) in the SI) from the calculation of the response function:

$$\Delta\nu = \frac{D_\psi k^2}{2\nu}\Sigma(k,\omega,\omega_{\tau_f}), \tag{3}$$

where, $\Delta\nu$ is the correction in ν due to non-linear terms in the equation for the ψ field, and $\nu = D_\psi k^2 + \phi_0 k^2 U(\mathbf{k})$. The self-energy term containing the two-loop contribution from the first order term (containing the two ψ fields in Eq. (S6) in the SI) determine the scaling laws of the observables in the intermediate time. In the long time limit, the long-range density fluctuations associated with the CCs determine the dynamical properties of TPs through CC-TP $\phi\psi$ fields in the fictitious time equation for the ψ variable. We use Eq. (3) to derive the scaling laws for the dynamical observables associated with the TPs.

Simulations: In order to test the theoretical predictions, we simulated a three dimensional MCS with embedded, mobile TPs. As in our previous studies, [12, 14, 15], we used an agent-based model to simulate

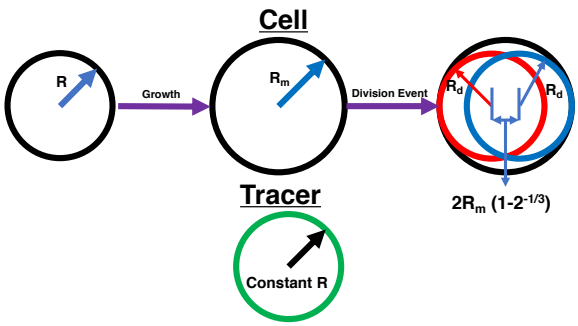

Figure 1: Schematic showing the difference between the CCs (black circle) and TPs (green circle). The CCs undergo growth and division. When the CCs divide they produce two daughter cells with $R_d = \frac{R_m}{2^{1/3}}$, and their relative position is displaced by $R_m(1 - \frac{1}{2^{1/3}})$ with their orientation being random with respect the sphere center. The TPs do not divide and their number is a constant in the simulations.

the dynamics of the TP-CC system. The cells are treated as interacting soft deformable spheres. The CC size increases with time, and divides into two identical daughter cells upon reaching a critical radius (R_m). The mean cell cycle time, measured in units of 15 hrs, is $\frac{1}{k_b}$. The CCs also undergo apoptosis at the rate k_a. However, the sizes and the number of the TPs are constant throughout the simulations.

To study the dynamics of TPs, we account for the CC-CC, CC-TP and TP-TP interactions. We model the interactions using two potentials (Gaussian and Hertz scheme) to ensure that the qualitative results are independent of the nature of the potential (See the details in the SI). The equation of motion governing the dynamics of TP and CCs is taken to be, $\dot{\vec{r}}_i = \frac{\vec{F}_i}{\gamma_i}$, where $\dot{\vec{r}}_i$ is the velocity of ith CC or TP, $\vec{F}_i$ is the force on i^{th} CC/TP, and γ_i represents the damping term (for details see reference [12]). The simulations are performed in the over-damped limit (see [12] and the SI for details).

We used a pressure inhibition mechanism (see the details in SI) to model the observed growth dynamics [12] of the MCS. The CCs can be either dormant or in the growth phase depending on the local microenvironment, which in our model is taken to be the pressure on the ith cell. Figure 1 shows the schematic of growth and division process of the CCs in the absence of the TPs. We argue later that the division event and the subsequent placement of the daughter cells (radius R_d) randomly in space adds a degree of stochasticity in the dynamics of the CCs. We initiated the simulations with 100 TPs and 100 CCs. The spatial coordinates of CCs and TPs were sampled using a normal distribution with mean zero and standard deviation 50 μm.

Results: Both theory and simulations predict that in the limit $t < \frac{1}{k_b}$, the TPs exhibit subdiffusive behavior. The non-linear term $\nabla \cdot \left(\psi(\mathbf{r},t) \int d\mathbf{r}' \psi(\mathbf{r}',t) \nabla U(\mathbf{r}-\mathbf{r}')\right)$ governs the scaling laws. In the spirit of self-consistent mode coupling theory, we replace ν by $\Delta\nu$ in the self-energy term $\Sigma(\mathbf{k},\omega,\omega_{\tau_f})$ (Eq.(3)). The momentum count of Eq. (3) with the self-energy term $\Sigma(\mathbf{k},\omega,\omega_{\tau_f})$ (see Fig. (S6a) in the SI) determines the dynamic exponent $z = 2 + \frac{d}{2}$.

The single cell mean-square displacement (MSD) behaves as, $\Delta(t) =< [r(t) - r(0)]^2 >\sim t^{2/z} = t^{\beta}$. In 3D, $\beta^T_{TP} = \frac{4}{7} = 0.57$ (the superscript T denotes theory), implying that the TPs undergo sub-diffusive motion, which is a characteristic feature of abiotic glass forming systems. The scaling exponent β^T_{TP} depends (explained in the SI) on the form of the interaction potential, which shows that the behavior of MSD in the intermediate time limit is non-universal.

We also simulated the motion of the TPs in a tumor spheroid, and calculated $\Delta_{TP}(t) = \langle[\mathbf{r}(t) - \mathbf{r}(0)]^2\rangle$ for both the interaction schemes (Gaussian and Hertz potential), using agent-based models. We tracked the positions of all the TPs, and calculated $\Delta_{TP}(t)$ by averaging over $\approx$ 2000 trajectories. Figure 2 shows $\Delta_{TP}(t)$ using the Gaussian potential and figure S2a in the SI shows $\Delta_{TP}(t)$ using the Hertz scheme. For both the potentials, we observe similar behavior. The plateau in figure 2 increases as the cell cycle time (τ), increases in the intermediate time regime ($t < \tau_{min}$). We find that $\Delta_{TP} \sim t^{\beta^S_{TP}}(\beta^S_{TP} = 0.11$ - the superscript S stands for simulations). Although both theory and simulations produce subdiffusive behavior there is a quantitative difference between β^S_{TP} and β^T_{TP}.

Interestingly, in the limit $t > \frac{1}{k_b}$, theory and simulations predict hyper-diffusive dynamics $\Delta_{TP} \sim t^{\alpha_{TP}}$ with $\alpha_{TP} > 2$. The effect of non-linearity due to the TP-CC interactions coupled with cell birth-apoptosis processes determine the long-time behavior of the TPs. The corresponding self-energy term in Eq.(3), giving rise to the hyper-diffusive dynamics, is shown in Fig.(S6c) in the SI. The momentum count of Eq. (3) with the self-energy term $\Sigma(\mathbf{k},\omega,\omega_{\tau_f})$ (see Fig.(S6c) in the SI) determines the MSD exponent, which is found to be $\alpha^T{}_{TP} = 2.28$. The self energy term $\Sigma(\mathbf{k},\omega,\omega_{\tau_f})$ (Fig(S2c) in the SI) depends linearly on the birth rate for the CCs. The different values for the cell cycle time, i.e., the different values of birth rates do not change the scaling of the self energy term. It only changes the coefficients of the self energy term. Therefore, the MSD exponent for the TPs is independent of the cell cycle time in the long time limit.

The simulation results are in excellent agreement with the theoretical predictions. For times exceeding the cell cycle time, ($t > \tau_{min}$), we observe hyper-diffusive behavior for the dynamics of TPs (see figure 2). For the Gaussian potential, we obtain the MSD exponent $\alpha^S_{TP} \approx 2.3$ (see the inset in figure 2) for the cell cycle time of $0.5\tau_{min}$, τ_{min} and $2\tau_{min}$. Therefore, both theory and simulations show that the TP undergoes hyper-diffusive motion in the long-time limit with α_{TP} being independent of τ_{min}.

The transition from sub-diffusive to hyper-diffusive motion is not sharp (see figure 2). The linear term in the non-linear growth profile ($\propto \phi(\phi_0 - \phi)$) contributes to the

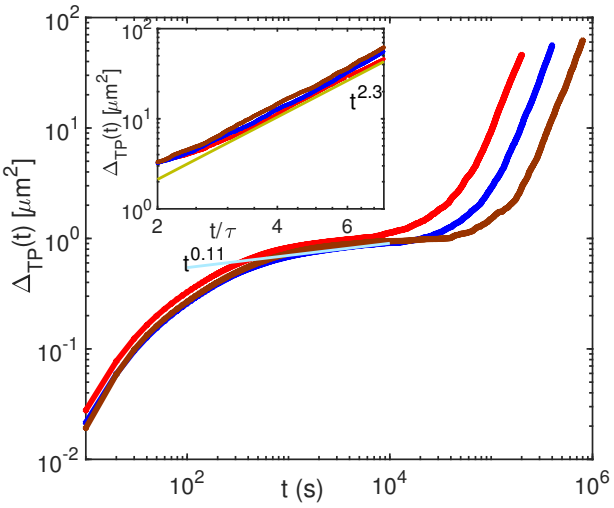

Figure 2: The mean-square displacement of TPs (Δ_{TP}) using the Gaussian potential.The curves are given for 3 different cell cycle time (red ($\tau = 0.5\tau_{min}$), blue ($\tau = \tau_{min}$), and brown ($\tau = 2\tau_{min}$) where $\tau_{min} = 54,000s$). Time to reach the hyper-diffusive behavior, which is preceded by a sub-diffusive regime (i.e $\Delta_{TP} \sim t^{\beta}, \beta^S_{cc}$= 0.11, shown by the cyan line), increases on increasing τ. In the $t > \tau$ limit, we observe hyper-diffusion. The inset shows Δ_{TP} for the three curves focusing on the hyper-diffusive regime. The x-axis of the inset plot has been scaled by $\frac{1}{\tau}$. The green line in the inset shows the exponent α^S_{TP}= 2.3.

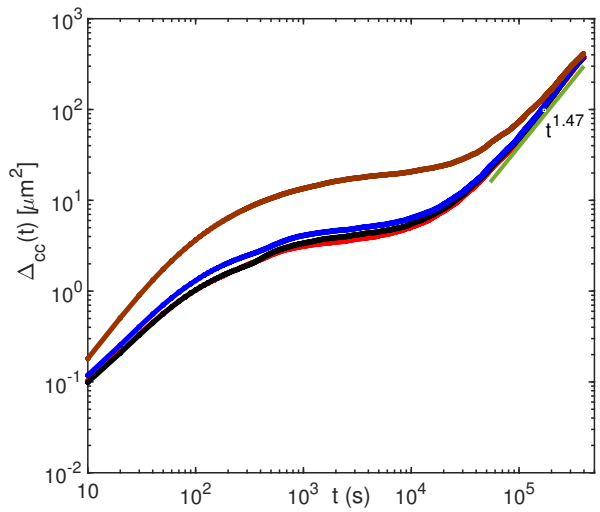

Figure 3: Dynamics of the CCs in the presence of the TPs. The mean-square displacement of the CCs (Δ_{CC}) using the Hertz potential. From top to bottom the curves correspond to different TP radius (brown - $r_{TP} =$ 2 r_c, blue - $r_{TP} = r_c$, and black - $r_{TP} = 0.75r_c$, and red - $r_{TP} = 0.5r_c$ (appears to be hidden), where $r_c = 4.5\mu m$ corresponds to the average cell radius). The green line serves as a guide to eye for exponent equal to $\alpha^S_{CC} = 1.47$.

TP motion in the transition region, and subsequently the non-linear term in the growth profile determines the dynamics of the TPs in the long-time limit. The momentum count of Eq. (3) with the self-energy term $\Sigma(\mathbf{k}, \omega, \omega_{\tau_f})$ (see Fig. (S2b) in the SI) determines the MSD exponent $\alpha^T_{TP} = 1.33$, implying super-diffusive motion. Therefore, the theoretical result validates the simulations in predicting smooth fluidization transition (Fig.(2)). In the absence of TPs, the birth-apoptosis processes determine the dynamics in CCs. The corresponding MSD exponent $\alpha_{CC} = 1.33$ [13]. In presence of TPs, the CCs exhibit super-diffusive motion with MSD exponent $\alpha^T_{CC} = 1.45$, which is in agreement with the simulation result (figure 3).

Theory and simulations show that α_{TP} exceeds α_{CC}, which we explain by examining the wave vector (k) dependence of the effective diffusion coefficient. For homogeneous systems, without birth or apoptosis, the density obeys Eq.(1) without the non-linear terms. The equilibrium fluctuations ($< \delta\psi(k,t)\delta\psi(k,0) >= \psi_0 \exp[-Dk^2t]$) are short-ranged. The diffusion-coefficient (D) is a constant and the MSD exponent is unity. The relaxation time for the time correlation function scales as k^{-z}, with $z = 2$. The deviation from this scaling would be indicative of anomalous diffusion. If we turn on the interactions (short-ranged) between the particles, the intensity of the equal time fluctuations diverges as k^{-z}, the fluctuations become long-ranged, and non-local extending over the size of the system. In this case, D is k dependent, scaling as k^{z-2}. This is the origin of the anomalous diffusion found here. Depending on the value of z, the CCs and the TPs could exhibit sub or hyper-diffusive motion. The non-linear term in Eq. (1) for the TP-TP interactions renormalizes the diffusion coefficient D. In the intermediate time the correlation function in real space $< \delta\psi(\mathbf{r}_1)\delta\psi(\mathbf{r}_2) >$ diverges as $r^{0.5}$ at large separation $r = |\mathbf{r}_1 - \mathbf{r}_2|$. The entire system becomes correlated. The relaxation time for the dynamic structure factor diverges as $k^{-3.5}$, implying that $z = \frac{7}{2}$, resulting in sub-diffusive motion (MSD exponent $\beta^T_{TP} = \frac{2}{z} = \frac{4}{7} \approx 0.57$). The stochastic birth-apoptosis process induces long-range non-equilibrium density fluctuations, which diverge as $k^{-3/2}$, which in turn induces TP density fluctuations ($\sim k^{-7/8}$) through TP-CC interactions. Thus, birth and apoptosis processes produce a dramatic change in the TP density fluctuations (from $k^{-3.5}$ to $k^{-7/8}$). As a result, the MSD exponent $\alpha^T_{TP} \approx \alpha^T_{TP} = 2.28$ in the long-time limit. On the other hand, the presence of TP induces only a minor change in the density fluctuations in the CCs ($\sim k^{-11/8}$). Accordingly, the diffusion coefficients $D_{CC} \sim k^{-5/8}$ for CC and $D_{TP} \sim k^{-9/8}$. The relaxation time associated with the time correlation functions for TPs ($k^{-7/8}$) is small compared to the degree of relaxation time for CCs ($k^{-11/8}$), which implies a higher degree of anomalous diffusion for the TPs.

A mechanistic explanation for $\alpha_{TP} > \alpha_{CC}$ in the long time limit can be gleaned from the simulations. To il-

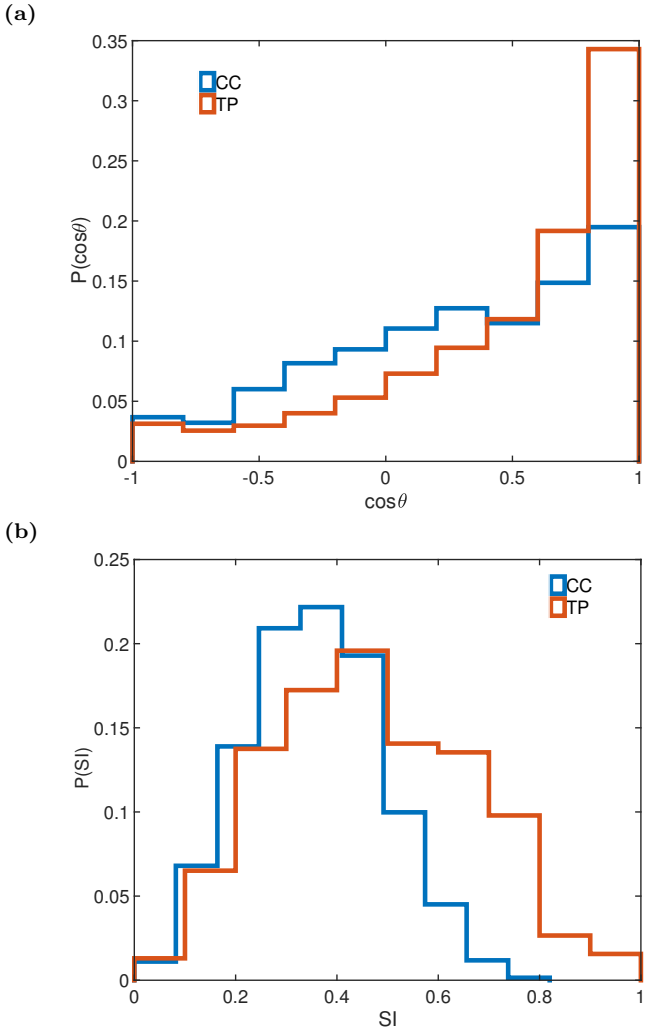

Figure 4: **(a)** Distribution of $\cos(\theta)$ for the TPs and CCs, where θ is the angle between two consecutive steps along a trajectory. The orange (blue) plot is for TPs (CCs). The distribution is skewed in the positive side (i.e $\cos(\theta) > 0$ indicative of persistent motion. However, the skewness is more for TPs than CCs and therefore $\alpha_{TP} > \alpha_{CC}$. **(b)** Distribution of Straightness Index (SI) which measures the rectilinearity of a trajectory. The orange (blue) plot is for TPs (CCs) which shows that the trajectory of TPs is more rectilinear compared to CCs.

lustrate the difference between the dynamics of the TPs and CCs, we calculated the angle (θ) between the trajectory of a CC between two consecutive steps. We define $\cos(\theta(t,\delta t)) = \frac{\delta\mathbf{r}(t+\delta t)\cdot\delta\mathbf{r}(t)}{|\delta\mathbf{r}(t+\delta t)||\delta\mathbf{r}(t))|}$, where $\delta\mathbf{r}(t) = \mathbf{r}(t+\delta t) - \mathbf{r}(t)$. Figure 4a shows the distribution of an ensemble and time averaged $\cos\theta$ for $\frac{\delta t}{\tau} = 1$. In the absence of any directed motion of the CCs and TPs the distribution of $\cos\theta$ would be uniformly distributed from -1 to 1. However, Figure 4a shows that $P(\cos\theta)$ is skewed towards unity implying that the motion of the TPs and CCs is persistent. As a result of the directed movement, the motion is hyper-diffusive (superdiffusive) for the TPs (CCs). Because the skewness is more pronounced for the TPs compared to the CCs (Figure 4a) it follows that $\alpha_{TP} > \alpha_{CC}$ in the long time limit.

To further demonstrate that the trajectories of the TPs are more persistent than the CCs, we calculated the Straightness Index (SI), $SI_i = \frac{\mathbf{r}_i(t_f)-\mathbf{r}_i(0)}{\sum\delta\mathbf{r}_i(t)}$. The numerator $\mathbf{r}_i(t_f)-\mathbf{r}_i(0)$ is the net displacement of ith TP or CC, and denominator $\sum\delta\mathbf{r}_i(t)$ is the total distance traversed. Figure 4b clearly demonstrates that TPs trajectories are more straight or persistent over longer duration. The physical reason for the distinct dynamical property of the TPs and CCs is because the CCs undergo proliferation and division. During each cell division, the CCs are placed randomly causing their trajectories to be less persistent. Consequently, $\alpha_{TP} > \alpha_{CC}$, which is predicted by theory and confirmed in the simulations.

Summary: In the present study, using both theory and simulations we probed the out of equilibrium dynamics of TPs embedded in a growing MCS containing cancer cells that undergo cell division and apoptosis. As a consequence of the self-generated active forces due to the CCs the evolving system is driven far away from equilibrium, which in turn produces unexpected and distinct dynamics in the CCs and TPs. We conclude with a few comments. (i) Using a theoretical framework and extensive off-lattice simulations we revealed the complex dynamical properties of both the TPs and CCs in the finite as well as in the long-time limit. The TP-TP interactions determine the sub-diffusive motion in the intermediate times. Interestingly, the long time hyper-diffusive motion of the TPs is a consequence of the biologically relevant events associated with the CCs. Simulations and theory show continuous change from sub-diffusive to hyper-diffusive motions for the TPs. The linear-dependence of the relaxation time on cell-cycle time shows stronger caging effect for higher values of cell-cycle times. The long-time exponent is non-universal, depending on the nature of the interactions. (ii) Although the interactions used in theory and simulations are different the excellent agreement between their predictions, especially in the long time limit, suggests that what determines the collective migration of the CCs is the overall growth law governing tumor expansion. The logistic growth of the tumor arising, in theory, is consistent with what we find in simulations over a range of times, which explains the predicted consistency between theory and simulations. We expect that the dynamics could change dramatically if the tumor growth law is altered, which can be accomplished by changing the ratio of birth and death rates. (iii) Perhaps, most importantly the present work shows that much about the long term dynamics of a collection of CCs could be learned by tracking the movements of embedded inert tracer particles because they do not perturb the CC movements significantly.

Acknowledgements This work is supported by the National Science Foundation (PHY 17-08128 and CHE 16-32756), and the Collie-Welch Chair through the Welch

Foundation (F-0019).

[1] P. Friedl and D. Gilmour, *Nat. Rev. Mol. Cell Biol.*, 2009, **10**, 445.

[2] M. Shaebani, A. Wysocki, R. Winkler, G. Gompper and H. Rieger, *Nat. Rev. Phys.*, 2020, **2**, xxx–xxx.

[3] S. Kumar and V. M. Weaver, *Cancer Metastasis Rev.*, 2009, **28**, 113–127.

[4] B. Desoize and J.-C. Jardillier, *Crit. Rev. Oncol. Hemat.*, 2000, **36**, 193–207.

[5] S. Walenta, J. Doetsch, W. Mueller-Klieser and L. A. Kunz-Schughart, *J Histochem Cytochem.*, 2000, **48**, 509–522.

[6] J. Laurent, C. Frongia, M. Cazales, O. Mondesert, B. Ducommun and V. Lobjois, *BMC cancer*, 2013, **13**, 73.

[7] A. M. J. Valencia, P.-H. Wu, O. N. Yogurtcu, P. Rao, J. DiGiacomo, I. Godet, L. He, M.-H. Lee, D. Gilkes, S. X. Sun *et al.*, *Oncotarget*, 2015, **6**, 43438.

[8] R. Richards, D. Mason, R. Levy, R. Bearon and V. See, *bioRxiv*, 2018, 443648.

[9] N. Martino, S. J. Kwok, A. C. Liapis, S. Forward, H. Jang, H.-M. Kim, S. J. Wu, J. Wu, P. H. Dannenberg, S.-J. Jang *et al.*, *Nat. Photonics*, 2019, **13**, 720–727.

[10] Y. L. Han, A. F. Pegoraro, H. Li, K. Li, Y. Yuan, G. Xu, Z. Gu, J. Sun, Y. Hao, S. K. Gupta *et al.*, *Nat. Phys.*, 2019, 1–8.

[11] A. Palamidessi, C. Malinverno, E. Frittoli, S. Corallino, E. Barbieri, S. Sigismund, G. V. Beznoussenko, E. Martini, M. Garre, I. Ferrara *et al.*, *Nat. mater.*, 2019, 1–12.

[12] A. N. Malmi-Kakkada, X. Li, H. S. Samanta, S. Sinha and D. Thirumalai, *Phys. Rev. X*, 2018, **8**, 021025.

[13] H. S. Samanta and D. Thirumalai, *Phys. Rev. E*, 2019, **99**, 032401.

[14] A. Malmi-Kakkada, X. Li, S. Sinha and D. Thirumalai, *arXiv preprint arXiv:1906.11292*, 2019.

[15] S. Sinha, A. Malmi-Kakkada, X. Li, H. Samanta and D. Thirumalai, *bioRxiv*, 2019, 842930.

[16] M. C. Marchetti, J.-F. Joanny, S. Ramaswamy, T. B. Liverpool, J. Prost, M. Rao and R. A. Simha, *Rev. Mod. Phys.*, 2013, **85**, 1143.

[17] C. Bechinger, R. Di Leonardo, H. Löwen, C. Reichhardt, G. Volpe and G. Volpe, *Rev. Mod. Phys.*, 2016, **88**, 045006.

[18] S. K. Nandi, R. Mandal, P. J. Bhuyan, C. Dasgupta, M. Rao and N. S. Gov, *Proc. Natl. Acad. Sci.*, 2018, **115**, 7688.

[19] M. Rauzi and P.-F. Lenne, in *Curr. Top. Dev. Biol.*, Elsevier, 2011, vol. 95, pp. 93–144.

[20] M. S. Hutson, Y. Tokutake, M.-S. Chang, J. W. Bloor, S. Venakides, D. P. Kiehart and G. S. Edwards, *Science*, 2003, **300**, 145–149.

[21] Y. Boucher, L. T. Baxter and R. K. Jain, *Cancer Res.*, 1990, **50**, 4478–4484.

[22] H. Fadnes, R. Reed and K. Aukland, *Microvas. Res.*, 1977, **14**, 27–36.

[23] O. Campàs, T. Mammoto, S. Hasso, R. A. Sperling, D. O'connell, A. G. Bischof, R. Maas, D. A. Weitz, L. Mahadevan and D. E. Ingber, *Nat. Methods*, 2014, **11**, 183.

[24] M. E. Dolega, M. Delarue, F. Ingremeau, J. Prost, A. Delon and G. Cappello, *Nat. Commun.*, 2017, **8**, 14056.

[25] A. Doostmohammadi, S. P. Thampi, T. B. Saw, C. T. Lim, B. Ladoux and J. M. Yeomans, *Soft Matter*, 2015, **11**, 7328–7336.

[26] G. Parisi and Y. S. Wu, *Sci. Sin.*, 1981, **24**, 484.

[27] H. S. Samanta, J. K. Bhattacharjee and D. Gangopadhyay, *Phys. Letts. A*, 2006, **353**, 113.

[28] H. S. Samanta and J. K. Bhattacharjee, *Phys. Rev. E*, 2006, **73**, 046125.

[29] D. S. Dean, *J. Phys. A*, 1996, **29**, L613.

[30] C. Doering, C. Mueller and P. Smereka, *Physica A*, 2003, **325**, 243.

[31] A. Gelimson and R. Golestanian, *Phys. Rev. Lett.*, 2015, **114**, 028101.

[32] H. S. Samanta, M. Hinczewski and D. Thirumalai, *Phys. Rev. E*, 2017, **96**, 012406.

[33] M. Doi, *J. Phys. A: Math. Ge.*, 1976, **9**, 1465.

[34] L. Peliti, *J. Phys. (France)*, 1985, **46**, 1469.